# Analytic Model for Halo Formation in High Current Ion Linacs

Robert L. Gluckstern
*Physics Department, University of Maryland, College Park, Maryland 20742*
(Received 8 March 1994)

We construct an azimuthally symmetric 2D model for halo formation in high current ion linacs. The driving term, a "breathing" oscillation caused by a transverse mismatch along the linac, leads to growth of ion amplitudes in the core through the parametric resonance. As the ion amplitude grows, its wave number increases, enhancing the resonance. This leads to the formation of a halo surrounding the core. We explore the dependence of this mechanism on the tune depression and the size of the mismatch. The model agrees well with simulations at Los Alamos, but does not yet include the effects of chaos observed in the simulations as the tune depression becomes severe.

PACS numbers: 41.85.−p, 29.17.+w, 29.27.Bd

*I. Introduction.*—High current, high duty factor ion linacs have become increasingly attractive in recent years. Among possible applications are heavy ion drivers for thermonuclear energy production, production of tritium, transmutation of radioactive wastes, and production of radioactive isotopes for medical use.

Obviously, it is desirable to accelerate the maximum possible current in such linacs. Much work has been done to explore the optimum transverse phase space distribution in such beams. In particular, the Kapchinsky-Vladimirsky (K-V) distribution [1] is simplest to analyze, since this projection into real space has a uniform density and therefore linear space charge forces. The stability of the K-V distribution has been analyzed and approximately confirmed by numerical simulations. Nevertheless it appears that, particularly at high currents, the K-V and other equilibrium distributions evolve to ones with rounded edges and tails. In many cases involving high peak current, the distribution spins off a cluster of particles in the form of a halo surrounding a dense core. This halo is seen in simulations as well as in actual linacs, such as LAMPF [2]. And efforts to remove the halo by collimation have been largely unsuccessful since the halos almost always regenerate.

It is clear that the halos will produce unacceptably high levels of radioactivity in high current, high duty factor linacs. For this reason considerable effort has recently been devoted to exploring their detailed structure and understanding the mechanism or mechanisms by which the halos are produced [3–6]. What has been learned is that halos are most likely to be produced at transition locations, such as where there are discontinuities in frequency, structure geometry, transverse focusing pattern, accelerating gradient and phase, etc.

In the present paper, we propose an analytic model for halo formation which appears to reproduce the main features seen in simulations and in actual linacs. In particular we consider a circular cw beam with a K-V core distribution and explore the motion of individual ions passing through the core. Since energy transfer between ions and the core can take place only if the core has a time dependent behavior, we consider the driving mechanism to be a "breathing" oscillation of the core. We then explore the resonant (parametric) interaction between the breathing core and the ions oscillating about and through the core. Of particular importance is the dependence of the frequency of each oscillating ion on its amplitude, which is related to the fraction of the oscillation for which the ion is within the core.

In spite of the fact that the actual distribution will have nonlinear fields, the use of a K-V distribution for the analysis leads us to a very likely mechanism for the development of the halo. In particular, the results provide an explanation for the low density region around the core which is surrounded by a somewhat higher density halo ring. This explanation will probably still apply for other self-consistent distributions.

*II. Model.*—We consider an azimuthally symmetric K-V core of radius $a$ for which the equation of motion of an ion is

$$x'' + k^2 x = x\begin{Bmatrix} \kappa/a^2, & r \le a \\ \kappa/r^2, & r \ge a \end{Bmatrix}, \tag{2.1}$$

where the prime stands for $d/dz$, and $k$ is the wave number of the transverse motion in the absence of space charge. The perveance of the beam, $\kappa = eI/2\pi\epsilon_0 m v^3$, is a dimensionless parameter proportional to the current $I$, where $e$, $m$, and $v$ are the charge, mass, and ion velocity, and $\epsilon_0$ is the permittivity of free space. The equation for $y$ is identical to Eq. (2.1).

We now assume a core oscillation of wave number $p$ of the form $a \to a(1 - \epsilon\cos pz)$ and expand $a^{-2}$ in Eq. (2.1) to first order in $\epsilon$, the relative oscillation amplitude. After some algebra, Eq. (2.1) can be written as

$$x'' + q^2 x = -\frac{\kappa}{a^2} x\left(1 - \frac{a^2}{r^2}\right)\Theta(r - a) + \frac{2\epsilon\kappa}{a^2} x\cos pz\,\Theta(a - r), \tag{2.2}$$

where $\Theta(u) = 1,0$ for $u > 0, u < 0$ and where $q = \sqrt{k^2 - \kappa/a^2}$ is the wave number of oscillations within the core.

0031-9007/94/73(9)/1247(4)$06.00

With the radial forces of Eq. (2.2), we see that the angular momentum $Lqa^2 \equiv xy' - x'y = r^2\theta'$ is constant. The equation for radial motion then becomes

$$r'' + q^2\left(r - \frac{L^2a^4}{r^3}\right) = -\frac{\kappa}{a^2}r\left(1 - \frac{a^2}{r^2}\right)\Theta(r - a) + 2\frac{\epsilon\kappa}{a^2}r\cos pz\,\Theta(a - r). \tag{2.3}$$

The first term on the right makes the oscillation wave number depend on amplitude and the second allows for energy transfer between the core and the oscillating ion.

In order to understand the role of the different terms in Eq. (2.3), we construct a simplified model by setting $L = 0$ and invoking a pendulum model for the first term on the right side of Eq. (2.3) by replacing $r(1 - a^2/r^2)\Theta(r - a)$ by $r^3/a^2$, corresponding to the cubic nonlinear term for a pendulum. (However, its sign is opposite from the conventional pendulum since, in our model, the wave number *increases* with increasing amplitude.) In addition, we extend the driving term to all values of $r$. The simplified equation for $x$ is therefore

$$x'' + q^2x = -\frac{\kappa}{a^2}\frac{x^3}{a^2} + 2\frac{\epsilon\kappa}{a^2}x\cos pz. \tag{2.4}$$

We now use the phase-amplitude method by writing $x/a = A\sin\psi$, $x'/a = qA\cos\psi$, where $\psi = qz + \alpha$, implying $A'\sin\psi + A\alpha'\cos\psi = 0$. Here $A$ and $\alpha$ are taken to be the slowly varying amplitude and phase parameters of the ion oscillation. Substituting into Eq. (2.4) and solving for $A'$ and $\alpha'$ we obtain

$$A' = -\frac{\kappa A}{qa^4}[A^2\sin^3\psi\cos\psi - \epsilon a^2\sin 2\psi\cos pz], \tag{2.5}$$

$$\alpha' = \frac{\kappa}{qa^4}[A^2\sin^4\psi - 2\epsilon a^2\sin^2\psi\cos pz]. \tag{2.6}$$

We now average over all rapidly varying oscillatory terms with the exception of the one with wave number $2q - p$ (the parametric resonance) and obtain

$$A' = \frac{\epsilon\kappa}{2qa^2}A\sin\Psi, \tag{2.7}$$

$$\Psi' = (2q - p) + \frac{3\kappa}{4qa^4}A^2 + \frac{\epsilon\kappa}{qa^2}\cos\Psi, \tag{2.8}$$

where $\Psi = (2q - p)z + 2\alpha$ is the phase of this resonant interaction. One then finds that an integral of the motion exists, enabling us to write [7]

$$\epsilon\cos\Psi = \Delta - \frac{3}{8}w - \frac{C}{w}, \tag{2.9}$$

where $w = A^2/a^2$, $\Delta = q(p - 2q)a^2/\kappa$, and where the integration constant $C$ is determined by the initial values of $w$ and $2\alpha$. By resorting to the envelope equation we can show that $p^2 = 4q^2 + 2\kappa/a^2$ for the breathing mode, so that

$$\Delta = \frac{1}{1 + \sqrt{(1 + k^2/q^2)/2}}, \tag{2.10}$$

where $q/k$ is the tune depression caused by the space charge. In Fig. 1 we plot $\epsilon\cos\Psi$ vs $w$ for $q/k = 0.412$, $\Delta = 0.35$, and various values of $C$. For $\epsilon = 0.1$, the polar plot of $w$ vs $\Psi$ is shown in Fig. 2. It is clear that $Q$ is an unstable fixed point and that the origin and $S$ are stable fixed points. Figure 2 is equivalent to a "second order stroboscopic plot" for integral values of $pz/2\pi$, and contains the main features of the resonant interaction. Specifically, all trajectories starting within the inner separatrix (thick solid curve) bounded by $P$and $Q$ oscillate in stable orbits while any trajectory starting just outside will travel along the outer separatrix (thick dashed curve). For these particles, as the amplitude of motion grows the true oscillation wave number increases, enhancing the resonant term and *locking in* to the resonance. And the presence of a thin distribution of trajectories near the outer separatrix has the appearance of a halo in $x - y$ space at the radius corresponding to $R$ in Figs. 1 and 2.

We now drop the simplified model and return to Eq. (2.3). Although the algebra is far more complicated we eventually obtain a more accurate version of Eq. (2.9) with a very similar set of curves to those in Figs. 1 and 2. First we rewrite Eq. (2.3) for the variable $s = r^2/a^2$, obtaining

$$s'' - \frac{(s')^2}{2s} + 2q^2\left(s - \frac{L^2}{s}\right) = -\frac{2\kappa}{a^2}(s - 1)\Theta(s - 1) + 4\frac{\epsilon\kappa}{a^2}s\cos pz\,\Theta(1 - s). \tag{2.11}$$

Guided by the parametrization of the $x$ and $y$ motions separately, the amplitude-phase parametrization of the two-dimensional oscillation is written as

$$s = \frac{w^2 + L^2}{2w} - \frac{w^2 - L^2}{2w}\cos(2qz + \gamma). \tag{2.12}$$

Here $w$ and $\gamma$ are slowly varying amplitude and phase parameters which would be constant if the right side of Eq. (2.11) vanished. We now write

$$s' = q\frac{w^2 - L^2}{w}\sin(2qz + \gamma) \tag{2.13}$$

and use Eq. (2.11) and the required connection between $w'$ and $\gamma'$ implied by Eq. (2.13) to obtain explicit expressions for $w'$ and $\gamma'$. We then average over oscillations at

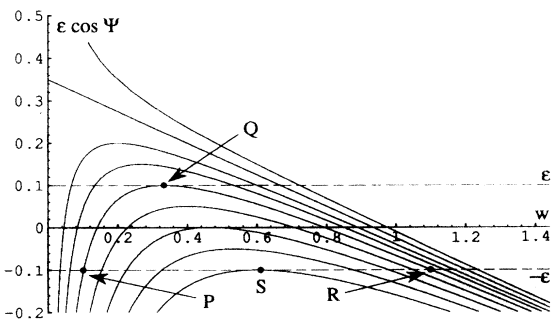


FIG. 1. Plot of $\epsilon\cos\Psi$ vs $w$ for the simplified model with $\Delta = 0.35$.

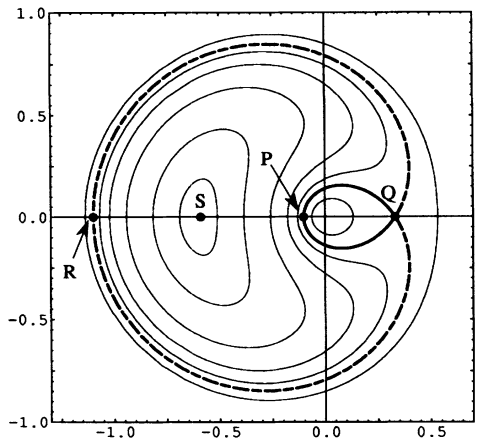


FIG. 2. Polar plot of $w$ vs $\Psi$ for the trajectories corresponding to the parametric resonance using $\Delta = 0.35$, $\epsilon = 0.1$, and the simplified model.

all wave numbers except $2q - p$, being careful to include the step functions as we obtain these averages. The final equations for $w'$ and $\Psi'$ [$\Psi = (2q - p)z + \gamma$] are similar to Eqs. (2.7) and (2.8) and again lead to an integral of the motion, which now is

$$g(1 - h)\epsilon \cos\Psi = f\Delta - t - C, \tag{2.14}$$

where $f(w) = (w^2 + L^2)/2w$, $g(w) = (w^2 - L^2)/2w$. Here

$$\pi h(w) = \tan^{-1}[\ell/(1 - f)] + \ell(1 - f)/2g^2 \tag{2.15}$$

for $w \geq 1$ and $\ell(w) = \sqrt{(w - 1)(w - L^2)/w}$. Also

$$t(w) = \frac{1}{\pi}\int_1^w \frac{dw}{wg}\left[(g^2 - f)\tan^{-1}\left(\frac{\ell}{1 - f}\right) + f\ell + L\tan^{-1}\left(\frac{2L\ell}{f - L^2}\right)\right], \tag{2.16}$$

for $w \geq 1$, and $h(w) = t(w) = 0$ for $w \leq 1$. The arctangents are taken to be in the first or second quadrant. The term in $b(w)$ comes from the amplitude dependence of the ion wave number. A more accurate expression for $b(w)$ can be obtained, if necessary, by solving Eq. (2.6) with $\epsilon = 0$.

Since the resonance will have its greatest effect when $L = 0$, corresponding to ion orbits which pass through the core center, we present a plot of $\epsilon \cos\Psi$ vs $w$ for $\Delta = 0.35$ and $L = 0$ in Fig. 3. The pattern of curves is very similar to that in Fig. 1, and the $w$, $\Psi$ polar plot in Fig. 4 for $\epsilon = 0.1$ has the same topology as for the simple model in Fig. 2, as is also the case for $L \neq 0$. But the scale for $w$ is about 7 times larger, corresponding to a detuning with amplitude about 7 times smaller than that given by the 3/8 factor in Eq. (2.14).

*III. Distribution of L in a symmetric K-V beam.*—The distribution in $L$ for a K-V beam is proportional to

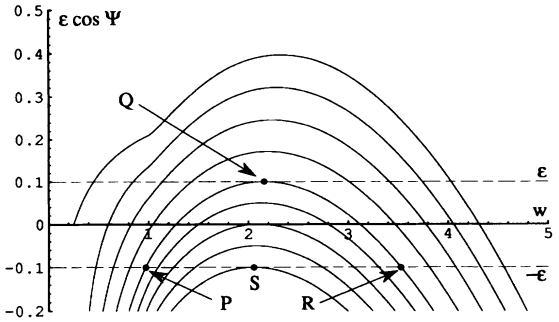


FIG. 3. Plot of $\epsilon\cos\Psi$ vs $w$ for the exact model with $\Delta = 0.35$, $L = 0$.

$$f(L) \sim \int\int\int\int dx\, dy\, dx'\, dy'\, \delta\Big(x^2 + y^2 + \frac{(x')^2}{q^2} + \frac{(y')^2}{q^2} - a^2\Big)\delta(x'y - xy' - Lqa^2). \tag{3.1}$$

We first do 45° rotations from the $x/a$, $y'/qa$ space to the $u$, $u'$ space and from the $y/a$, $x'/qa$ space to the $v$, $v'$ space and follow this by integrating over the polar angles in the $uv'$ and $vu'$ spaces. This leads to

$$f(L) \sim \int_0^\infty ds \int_0^\infty dt\, \delta(s + t - 1)\delta\Big(\frac{s - t}{2} - L\Big) = \begin{Bmatrix} 1, & 2|L| < 1 \\ 0, & 2|L| > 1 \end{Bmatrix}, \tag{3.2}$$

where $s = u^2 + (v')^2$ and $t = v^2 + (u')^2$ are both positive. Therefore the distribution in $L$ for a K-V beam is uniform from $L = -1/2$ to $L = 1/2$ and vanishes for $|L| > 1/2$.

*IV. Implications of the model.*—Since the breathing K-V beam is a solution of the Vlasov equation, particles within the core will continue to remain there, even in the presence of the resonant interaction. If however,

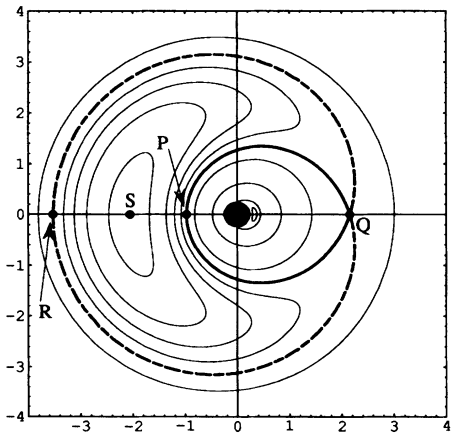


FIG. 4. Polar plot of $w$ vs $\Psi$ for the trajectories corresponding to the parametric resonance using $\Delta = 0.35$, $L = 0$, $\epsilon = 0.1$, and the exact model.

some other mechanism moves the particle outside the core, particularly to an oscillation amplitude exceeding that corresponding to the points $P$ or $Q$ in the figures, a halo will develop at a radius corresponding to point $R$ in the figures. The most likely mechanism to do this is an instability associated with a nonlinear density perturbation. In addition, simulations show that chaotic motion develops near point $Q$ in the figures for a large amplitude breathing mode at high current, enabling particles in the core to populate the halo.

*V. Summary and discussion.*—We considered a symmetric K-V beam undergoing a breathing mode and found that the parametric resonance ($2q = p$) is a vehicle for particles to leave the core of the beam and perform excursions to large amplitude, forming a distribution in real space in the form of a halo. In this calculation, we neglected the effect of high frequency terms, and the effect of other possible resonances and driving oscillations. Thus our model, which successfully describes a mechanism by which halos can and probably do form, is only an approximation to a much more complicated situation.

We have compared our predictions with some preliminary simulations performed for $L = 0$ by Wangler [8], and find that, for tune depressions from $q/k = 1$ to 0.6, the topology of the stroboscopic plot resembles Figs. 2 and 4 very closely. For tune depressions below 0.6, the stroboscopic plot shows the onset of chaotic behavior in an ever widening band near the inner separatrix as the tune depression deepens. Particles inside but near to the inner separatrix are then able to move outside the inner separatrix and participate more easily in the development of the halo.

Wangler's simulations using a K-V beam [8] confirm that core ions always remain within the inner separatrix. It is quite possible for core ions to lie outside the equivalent inner separatrix for nonuniform equilibrium charge density distributions. We therefore expect the halo mechanisms in the present model to apply to non-K-V beams as well. Lagniel's simulations [6] give similar results, showing the onset of chaos for high space charge as well as the similarity with the three-body astronomical problem.

Our present model is unable to describe either diffusion or chaos in the $w$, $\Psi$ phase space. If we were to try to do so we would have to include the neglected high frequency terms, as well as resonances other than the one corresponding to the parametric resonance. Integrals of the motion corresponding to Eq. (2.14) would no longer be valid. Descriptions of the growth of halos including the effects of chaos and diffusion will require further analysis and/or extensive numerical simulations.

The author would like to thank Alex Dragt, Bob Jameson, Pierre Lapostolle, Ron Ruth, Rob, Ryne, Fred Skiff, and Tom Wangler for several helpful comments. He is also indebted to Dan Abell for performing the calculations leading to Figs. 1–4.

[1] See I. M. Kapchinsky, *Theory of Resonance Linear Accelerators* (Harford Academic Press, New York, 1985), p. 247ff.

[2] R. A. Jameson, Los Alamos Report No. LA-UR-93-1209 (unpublished). Jameson describes the early observations of emittance growth and halo production, with particular reference to LAMPF simulations and observations.

[3] M. Reiser, in Proceedings of the 1991 Particle Accelerator Conference, San Francisco, California, (unpublished), p. 2497.

[4] A. Cucchetti, M. Reiser, and T. Wangler, in Proceedings of the 1991 Particle Accelerator Conference (Ref. [3]), p. 251.

[5] J. S. O'Connell, T. P. Wangler, R. S. Mills, and K. R. Crandall, in Proceedings of the 1993 Particle Accelerator Conference, Washington, D.C. (unpublished), p. 3657.

[6] J. M. Lagniel, Nucl. Instrum. Methods Phys. Res., Sect. A **345**, 46 (1994).

[7] This result can also be obtained using a contact transformation, followed by neglecting rapidly oscillating terms. In fact, the transformed Hamiltonian in the canonical variables $w$ and $\Psi$ is $H = (\kappa/qa^2)[w\epsilon\cos\Psi - \Delta w + 3w^2/8]$.

[8] Tom Wangler (private communication).

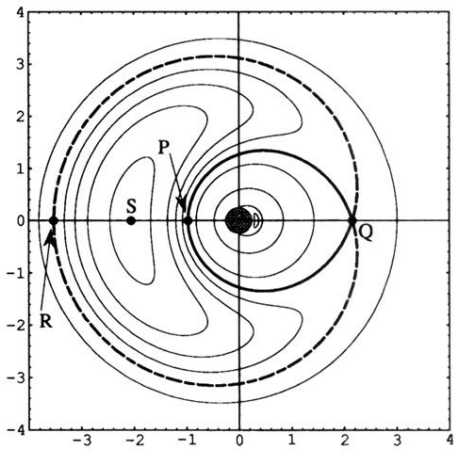


FIG. 4. Polar plot of $w$ vs $\Psi$ for the trajectories corresponding to the parametric resonance using $\Delta = 0.35$, $L = 0$, $\epsilon = 0.1$, and the exact model.